

DOI 10.24425/ae.2022.140717

Dynamic rating method of traction network based on wind speed prediction

ZHAOXU SU^{ORCID}, MINGXING TIAN[✉], LIJUN SUN, RUOPENG ZHANG*School of Automation and Electrical Engineering, Lanzhou Jiaotong University
China**e-mails: suzhaoxu@aliyun.com, [✉]tianmingxing@mail.lzjtu.cn, {442323513/302632699}@qq.com*

(Received: 01.09.2021, revised: 15.12.2021)

Abstract: The operating temperature of the transmission line in the traction network is affected by geographical and climatic factors, especially the wind speed. To make better use of the thermal stability transmission capacity of the traction power supply system in improving the short-term emergency transmission capacity, the dynamic rating technology is introduced into the traction power supply system. According to the time-varying characteristics of the actual wind speed, a dynamic rating method of the traction network based on wind speed prediction is proposed and constructed. Based on the time series model in predicting the wind speed series along the corridor of the traction network, the temperature curve of each transmission line under different currents is calculated by combining it with the heat balance equation of an IEEE-738 capacity expansion model, thus the relationship between the peak operating temperature and current of each transmission line in the prediction period is obtained. According to the current distribution coefficient, the capacity increase limit of the traction network is determined. The example shows that the proposed dynamic rating method based on wind speed prediction is an effective method to predict the short-term safe capacity increase limit of the traction network, which can increase the comprehensive capacity of the traction network by about 45% in the next six hours, and the capacity increase effect is obvious, which can provide reference and technical support for short-term emergency dispatching of traction power supply dispatching centres.

Key words: dynamic thermal rating, IEEE-738, short-term emergency dispatch, time series model, traction power supply, wind speed prediction

1. Introduction

With the increased railway transportation load and speed, the requirements for the thermal stable transmission capacity of the traction network are becoming higher. The thermal stable transmission capacity of the traction network will gradually become a new bottleneck restricting



© 2022. The Author(s). This is an open-access article distributed under the terms of the Creative Commons Attribution-NonCommercial-NoDerivatives License (CC BY-NC-ND 4.0, <https://creativecommons.org/licenses/by-nc-nd/4.0/>), which permits use, distribution, and reproduction in any medium, provided that the Article is properly cited, the use is non-commercial, and no modifications or adaptations are made.

the transportation capacity of the equipment [1]. The research shows that when considering the actual weather conditions, in most cases, the thermal stable transmission capacity of the transmission lines using dynamic line rating (DLR) technology can be improved by 20%–30% [2]. At the beginning of this century, DLR technology was introduced to East China's power grid, where the substantial economic and social benefits of this technology are proven [3]. At first, this technology was primarily applied in the public power system. Afterward, experts and scholars introduced the electro-thermal coupling theory into the traction power supply system combined with the particular network topology of the traction power supply system, revealing that the comprehensive current-carrying capacity of the traction network is closely related to its geographical and climatic conditions [4]. On this basis, this paper further introduced DLR into the traction power supply system to improve the thermal stable transmission capacity of the traction network, which has a good application prospect.

DLR technology calculates the maximum allowable current-carrying capacity according to different capacity increase models and meteorological parameters along the transmission line erection corridor. The thermal stability transmission capacity of the transmission line is related to many factors such as parameters, operating environment and corridor ground conditions, including wind speed, wind angle, ambient temperature, solar radiation and so on, especially the wind speed has a significant impact on the thermal stability transmission capacity of the transmission line. The wind speed has inevitable fluctuation characteristics in time and space scale. Reference [5] analyzed and calculated the 750 V transmission capacity of Shaanxi Province in China by obtaining meteorological data along the transmission line erection corridor by GIS and GRAPES. Reference [6] uses the consistency of some meteorological elements to establish the deviation probability model of meteorological data and calculate the maximum allowable carrying capacity of the transmission line. The previous line dynamic capacity increase technology only focused on the line capacity increase calculation. Still, the relevant research on the influence of time-varying characteristics of parameters such as wind speed on the existing dynamic capacity increase system of the traction network in practical application is not sufficient. The operation scheduling of the traction network needs to make decisions in advance. The maximum allowable current-carrying capacity calculated only based on the real-time data at that time cannot meet the actual needs of early decision-making. Although the meteorological prediction system has been gradually improved in recent two decades, it still has the limitations of short-term prediction deviation, high calculation cost, insufficient response time and spatial resolution [7]. With the advent of big data, using machine learning algorithms to predict the required data can effectively solve the above problems. Reference [8] proposed a short-term load forecasting model combining fuzzy exponential weighting and an improved harmonic search algorithm with high forecasting accuracy. From the perspective of optimization, the proposed algorithm has advantages. However, little reference predicts the wind speed parameters to master the thermal stability limit capacity in the capacity increase section.

A dynamic capacity increase method of the traction network based on wind speed prediction is proposed in this paper to solve the above problems. In consideration of predicting the short-term wind speed sequence along the traction network erection corridor based on the time series model and in combination with the heat balance equation, the short-term temperature change curve of each transmission line under different currents is calculated. The relationship between the predicted peak operating temperature of each transmission line and the current is quantitatively

analyzed and the short-term capacity increase limit of the traction network is dynamically checked, to reduce the adverse impact of wind speed time-varying characteristics on capacity increase limit evaluation. Finally, a detailed analysis and demonstration are carried out to verify the correctness and feasibility of the method proposed in this paper.

2. Equivalent circuit model of the traction network

The transmission conductor of the traction network generally includes contact and messenger wires and reinforcing wire is arranged in the high-speed and heavy load area [9, 10], as shown in Fig. 1.

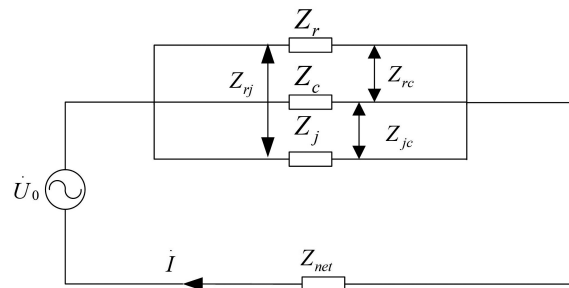


Fig. 1. Equivalent circuit model of transmission line in the traction network

Figure 1 shows a voltage phasor at a low voltage side of the traction substation, where \dot{U}_0 , Z_j , Z_c and Z_r represent the self-impedance of the contact line, messenger line and reinforcing line, respectively; Z_{rj} is the mutual-impedance between the reinforcing line and contact line; Z_{rc} is the mutual-impedance between the reinforcing line and messenger line; Z_{jc} is the mutual-impedance between the contact line and messenger line; Z_{net} is the unified equivalent impedance of the traction network which includes the impedance of the contact suspension of the traction substation and the impedance of the locomotive in the operation section and \dot{I} is the comprehensive current-carrying of the power supply circuit in the traction network. The specific calculation method of self-impedance and mutual impedance between lines in Fig. 1 is shown in References [9, 10].

The comprehensive current-carrying capacity of the traction network I_{max} can be expressed in (1).

$$I_{max} = \min \left\{ \frac{I_g^{max}}{k_g} \right\}. \quad (1)$$

The maximum allowable operating current-carrying capacity of the supporting comprehensive current-carrying capacity of each transmission line of the traction network I_{pt} can be calculated as:

$$I_{pt} = I_{max} k_g, \quad (2)$$

where: j , c and r can be taken in the power supply section with the reinforcing line, representing the contact line, messenger line and reinforcing line, respectively, and j and c can be taken in the section without the reinforcing line, representing the contact line and messenger line, respectively;

$I_{g \max}$ is the maximum allowable operating current-carrying capacity when the temperature of the transmission line g of the traction network reaches its maximum allowable operating temperature and is the current distribution coefficient of the g line.

3. Heat balance equation of the transmission line

The temperature of the transmission line in the traction network determines its transmission capacity. For the safe operation of the line, the line temperature shall not exceed the requirements of its design regulations to avoid damage to the line and affect the safety of the power supply. The line temperature is not a constant value and changes all the time, depending on the energy balance between the conductor's heat and surface heat exchange. The heat exchange is mainly affected by the temperature difference between the conductor and the environment and the external environment, such as wind speed, wind angle, altitude and solar radiation intensity. In consideration with Joule heat, the convective heat dissipation, radiation heat dissipation and solar radiation heat absorption of the transmission line, the dynamic capacity increase model of the transmission line in the traction network is established.

According to the IEEE-738 standard, the heat exchange process of the transmission conductor meets the transient heat balance equation shown in Eq. (3) [11, 12].

$$\frac{dT_s}{dt} = \frac{I^2 R(T_s) + q_s - q_c(T_s) - q_r(T_s)}{MC_p}, \quad (3)$$

where: M is the mass of the transmission line per unit length, kg/m; C_p is the specific heat capacity of the transmission line material, J/kg $^\circ$ C; T_s is the operating temperature of the transmission line, $^\circ$ C; q_c is the convective heat dissipation, W/m; q_r is the radiation heat dissipation and q_s is the solar radiation heat absorption, W/m.

The relationship between the transmission line resistance and temperature can be expressed as:

$$R(T_s) = R_{20} [1 + \alpha_l(T_s - 20)], \quad (4)$$

where R_{20} is the resistance value of the unit length transmission line at 20° and α_l is the resistance temperature coefficient.

The convective heat dissipation power q_c , radiant heat dissipation power q_r and solar radiation heat absorption power q_s satisfy Eqs. (5) to (7):

$$q_r(T_s) = 1.78D_0\varepsilon [(T_s + 273)^4 - (T_a + 273)^4] \cdot 10^{-9}, \quad (5)$$

$$q_s = \alpha Q_{se} \sin(\theta)A, \quad (6)$$

$$\begin{cases} q_{c1}(T_s) = K_{\text{angle}} \left[1.01 + 1.35 \left(\frac{D_0 \rho_f V_w}{\mu} \right)^{0.52} \right] k_f (T_s - T_a) \\ q_{c2}(T_s) = 0.754 K_{\text{angle}} \left(\frac{D_0 \rho_f V_w}{\mu} \right)^{0.6} k_f (T_s - T_a) \\ q_c(T_s) = \max(q_{c1}(T_s), q_{c2}(T_s)) \end{cases}, \quad (7)$$

where: K_{angle} is the wind direction coefficient (Pu); D_0 is the line radius (m); ρ_f is the air density (kg/m^3); V_w is the wind speed (m/s); μ_f is the air dynamic viscosity (kg/m/s); k_f is the air thermal conductivity ($\text{W/m}^\circ\text{C}$); T_a is the ambient temperature of the conductor ($^\circ\text{C}$); ε is the emissivity (Pu); α is the heat absorption coefficient of the line (Pu); Q_{se} is the solar radiation intensity (W/m^2); θ is the effective incidence angle of the sun (deg) and A is the effective projected area of the transmission line per unit length (m^2). The calculation formula is detailed in Reference [11] of K_{angle} , ρ_f , μ_f and Q_{se} .

When the heat absorption and dissipation of the transmission line reach dynamic balance, Eq. (3) becomes:

$$I^2 R(T_s) + q_s = q_c(T_s) + q_r(T_s). \quad (8)$$

Therefore, the maximum allowable operating current-carrying capacity of a single transmission line can be expressed as:

$$I_{T_{\max}} = \sqrt{\frac{q_c(T_{\max}) + q_r(T_{\max}) - q_s}{R(T_{\max})}}, \quad (9)$$

where T_{\max} is the maximum allowable operating temperature of a single transmission line.

From Eqs. (3) to (9), the thermal stability transmission capacity of the transmission line of the traction network is affected by the geographical and climatic parameters along the erection corridor of the traction network. According to the change of geographical and climatic parameters, the comprehensive current-carrying capacity of the traction network also changes. Wind speed has the most significant impact on the maximum allowable operating current-carrying capacity within a specific range, followed by wind direction, ambient temperature, sunshine intensity and altitude [13]. When the line parameters, maximum allowable operating temperature of the line and the ambient temperature are determined, the following can be assumed: the greater the wind speed, the greater the allowable operating ampacity.

Therefore, taking the comprehensive current-carrying capacity as the research object, the wind speed parameters as the core and the prediction model as the link, this paper puts forward the capacity increase limit evaluation method of the traction network based on wind speed prediction, which can dynamically evaluate the comprehensive current-carrying capacity of the traction network in the short term in real-time and calculate the thermal stability transmission capacity of the traction network in the short-term.

4. Wind speed prediction method based on time series model

References [14–16] proved that a time series model simulates and predicts wind speed and obtains good results. Therefore, wind speed prediction based on a time series model can be described as the historical wind speed data, which was built in the time series model to describe the statistical law of wind speed in the change process and established the corresponding expression of wind speed prediction to predict the short-term wind speed in the future.

Often, the wind speed series needs to be differential one to two times to meet the differential autoregressive moving average (ARMA) model. The specific difference formula is as follows:

$$\nabla^d x_t = (1 - B)^d x_t, \quad (10)$$

where: B is the backward operator, thus $Bx_t = x_{t-1}$; ∇ is the backward shift difference operator, thus $\nabla x_t = x_t - x_{t-1} = (1 - B)x_t$ and d is the order of difference, thus $\nabla^d = (1 - B)^d$.

The ARMA is constructed when the wind speed series meets the stability requirements. The current value of the model can be regarded as the finite weighted sum of the past values and its superposition with the finite weighted sum of past disturbances, that is:

$$x_t = \sum_{i=1}^p \varphi_i x_{t-i} + \varepsilon_t - \sum_{j=1}^q \theta_j \varepsilon_{t-j} \quad (t = 1, 2, \dots, N), \quad (11)$$

where: φ_i is the coefficient of the i -th autoregressive term; θ_j is the coefficient of the j -th moving average term; p and q represent the order of the autoregressive model and moving average model, respectively; ε_t is the random interference quantity that forms a normal white noise process, where the mean is 0 and the variance is σ_a^2 . Therefore, $\varepsilon_t \in N(0, \sigma_a^2)$.

The specific modelling process is detailed in References [14–16].

5. Calculation flow of dynamic capacity increase in short-term traction network based on wind speed prediction

The calculation flow of the traction network dynamic capacity increase method based on wind speed prediction is shown in Fig 2. The short-term prediction proposed in this paper mainly aims to predict model parameters along the traction network erection corridor in the next 1–24 hours. Therefore, this paper studies the dynamic capacity increasing method of the traction network considering the time-varying characteristics of wind speed. The implementation steps are as shown in Fig. 2.

Figure 2 shows the calculation flow of the traction network dynamic capacity increase method based on wind speed prediction. Given that the traction dispatching centre needs time to complete dispatching and safety verification, the short-term prediction proposed in this paper is mainly for the prediction of model parameters along the traction network erection corridor in the next 1–24 hours, and the obtained parameters can meet most of the time requirements of the traction dispatching centre. Therefore, this paper studies the dynamic capacity increasing method of the traction network considering the time-varying characteristics of wind speed. The implementation steps are as follows in Fig. 2.

Firstly, the traction dispatching centre performs initialisation operations that include inputting some basic parameter information of the transmission line of the traction network, setting the initial temperature of the conductor, setting the maximum allowable operating temperature of the transmission conductor, calculating the current distribution coefficient of the transmission conductor and so on. Secondly, a wind speed prediction model based on a time series is established based on the historical wind speed series of the meteorological centre. Hence, the short-term wind speed prediction sequence and different levels of current are combined with the transient heat balance equation to calculate the short-term temperature change curve of each transmission line. Afterward, the relationship between the predicted operating temperature peak and current of each transmission line in the prediction period is obtained. Finally, through the quantitative analysis of the relationship between the predicted operating temperature peak and current of each

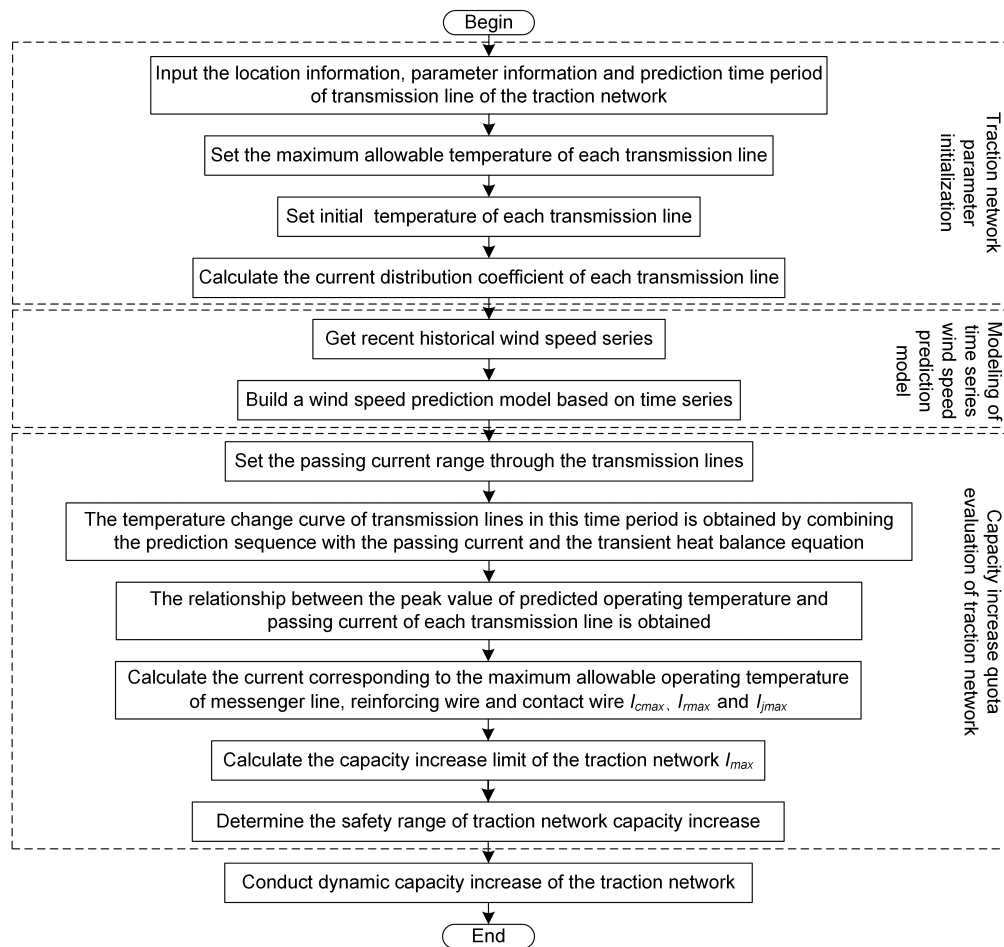


Fig. 2. Calculation process of short-term capacity increase in the traction network

transmission conductor, the current value corresponding to the maximum allowable operating temperature of each transmission line of the traction network and the comprehensive current-carrying capacity limit of the traction network in combination with the current distribution relationship are calculated, hence determining the safe capacity increases range and carries out short-term capacity increase.

6. Case study

Figure 3 shows the spatial location distribution when a single-line direct supply transmission line is erected in the Weiyuan section of Gansu Province of the Lanzhou Chongqing railway in China, where the selections of transmission lines are through CTAH120 contact wire, JTMH95

messenger wire and LGT 185/30 reinforcing wire. Table A.1 lists the specific parameters of the line. For example, the capacity increase limit of the traction network within six hours goes through a detailed calculation process.

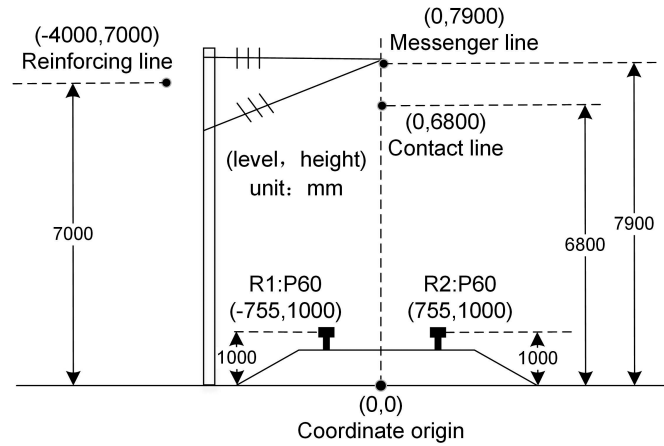


Fig. 3. Spatial distribution of transmission lines (unit: mm)

Because of the characteristics of the time series analysis method, this paper uses the 48-hour measured wind speed data of the Weiyuan meteorological station in Gansu Province of China from 7–9 January 2021. The sampling data is shown in Fig. 4. The data sampling interval is ten minutes, and the total length is 288. These wind speed data are divided into two groups. The first

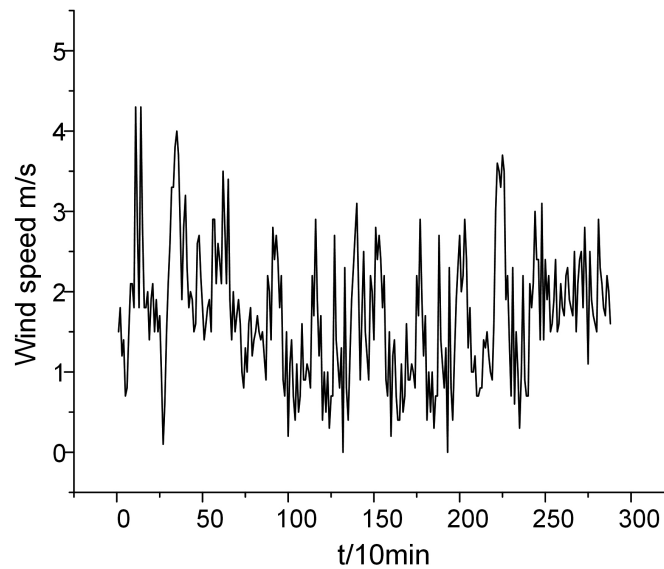


Fig. 4. Wind speed variation series in Weiyuan area in China

group uses the first 252 data (first 42 hours) to form a sample series for the modelling of a time series wind speed prediction model, while the second group uses the remaining 36 data (after six hours) as test data to compare with the predicted value, and selects the average absolute error MAE to analyse its prediction performance quantitatively.

6.1. Calculation of current distribution coefficient

In Reference [4], the equivalent depth of the current in the ground is taken by $D_g = 93000$ mm and uses the transmission line parameters (Table A.1) and the spatial relative position relationship of the transmission line of the traction network. The current distribution coefficient is calculated in Table 1.

Table 1. Current distribution coefficient of transmission line

Coefficient name	k_j	k_c	k_r
Value	0.337	0.316	0.348

6.2. Comparison of current-carrying capacity under different meteorological conditions

According to the 253rd wind speed acquisition time of the Gansu Weiyuan section from the Lanzhou Chongqing railway in China, the maximum allowable operating current-carrying capacity and comprehensive current-carrying capacity of the traction network of each transmission line of the traction network are calculated, as shown in Table 2. The calculation parameters are shown in the geographic and climatic parameter information in Table A.2.

Table 2. Maximum allowable operating current carrying capacity (A)/temperature ($^{\circ}$ C)/maximum capacity increase percentage of transmission lines in the traction network

Category	Factory value	Code meteorological conditions	Actual meteorological conditions	Maximum capacity increase percentage
Contact line	430/95	389/77	597/64	64%
Messenger line	366/95	366/95	562/95	53%
Reinforcing line	515/90	400/76	615/58	43%
Comprehensive current-carrying capacity	–	1158/–	1756/–	55%

The factory value of the maximum allowable operating current-carrying capacity of each transmission line is given in Table 2, which is the maximum allowable operating current-carrying capacity calculated under the meteorological conditions specified in the current technical regulations (wind speed of 0.5 m/s, wind angle at 90° , ambient temperature at 40° C, a sunshine intensity of $1000 \text{ W}\cdot\text{m}^2$, heat absorption coefficient at 0.9 and radiation coefficient 0.9). In the current trac-

tion network dispatching, the transportation limit is mainly used as the dispatching basis. Table 2 shows that the transmission current-carrying of each transmission line of the traction network is greatly affected by geographical and climatic conditions. The thermal stable transmission capacity calculated under the actual geographical and climatic conditions is much larger than the results calculated under the geographical and climatic environment specified in the design specification and has great excavation potential. For example, when the temperature of the messenger line reaches a limit of 95°C, the factory value of the maximum allowable operating current-carrying is 366 A. The regulations stipulate that the maximum allowable operating current-carrying under meteorological conditions is 366 A, while the current-carrying capacity under actual meteorological conditions can reach 562 A and can be increased by 53%. The comprehensive current-carrying capacity of the traction network under the meteorological conditions specified in the regulations is 1158 A, which can reach up to 1756 A under the actual meteorological conditions and can be increased by 55%. However, due to the prominent time-varying characteristics of the actual meteorological parameters, the comprehensive current-carrying capacity of the traction network calculated at this time cannot meet the requirements of the continuous and safe operation of the traction network.

6.3. Establishment of wind speed prediction model based on time series

6.3.1. Model recognition and stabilisation

In this paper, the unit root is used to test the collected wind speed series. Because no unit root in the collected wind speed series is obtained, the collected wind speed series is stable and stabilisation is not necessary.

The sequence autocorrelation function (ACF) and partial autocorrelation function (PACF) are shown in Figs. 5(a) and 5(b), respectively. According to the model judgment criteria, the first 252 wind speed data sequences collected in the Weiyuan section of Gansu Province are suitable for ARMA model prediction.

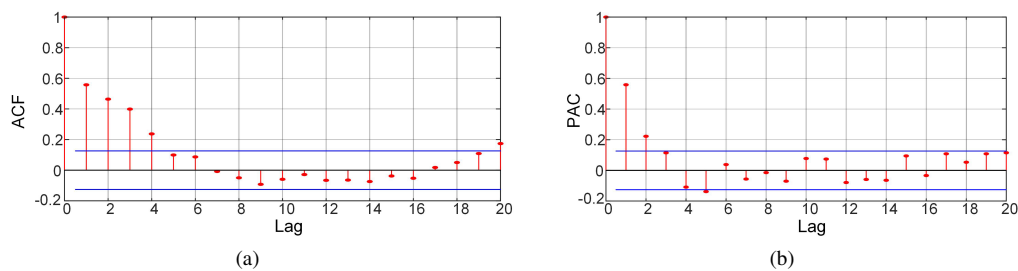


Fig. 5. (a) partial autocorrelation function (ACF); (b) sequence partial autocorrelation function (PACF)

6.3.2. Order determination and parameter solution of the model

After the unit root test of the sequence, the model category is determined. According to the autocorrelation and partial autocorrelation functions of the sequence and the principle of determining the order, the wind speed sequence p and q collected in the Weiyuan section of Gansu Province in China must be an integer within six.

The least square method is used to estimate the unknown parameters in the ARMA (p, q) model, and the group with the lowest Akaike information criterion (AIC) value is selected [17]. According to the AIC information criterion and considering the significance of parameters, the ARMA (4, 4) model is finally selected to fit the collected wind speed series. The specific parameters are shown in Table A.3. When p and q are 4 with $AIC = -0.597606$, the time series wind speed prediction model is the best fitting.

6.3.3. Residual sequence test

To check whether the residuals of the obtained ARMA model have autocorrelation characteristics, Fig. 6 shows the ACF of the residuals, in which the blue line indicates the limit of statistical significance, showing that most of the lagging autocorrelations are within the effective line. In addition, the Ljung box Q [18] statistic method is also used to test the white noise of the residual sequence to check whether the residual sequence is autocorrelated. No autocorrelation in the residual sequence was obtained based on the test results.

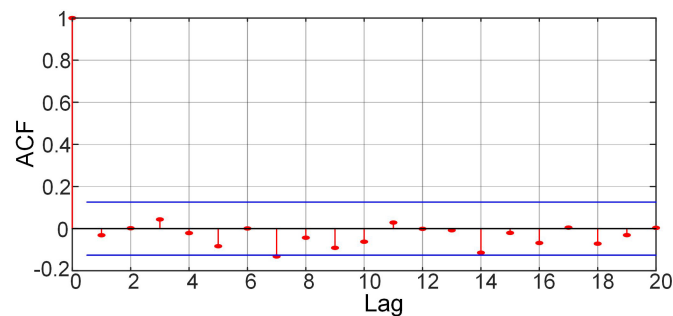


Fig. 6. Autocorrelation function of residual sequence (ACF)

The histogram of the residual sequence is shown in Fig. 7. The dotted line is the probability density function of the standard normal distribution, which indicates that the residual sequence is close to the normal distribution. Therefore, the residual is very close to the Gaussian white noise,

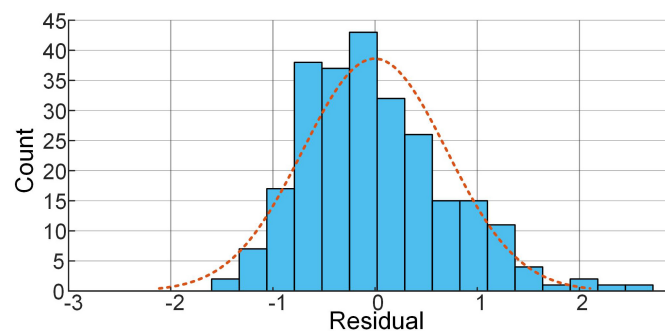


Fig. 7. Histogram of residuals

and its average absolute error MAE is 0.3628, indicating the reliability of the time series model for predicting the wind speed series.

6.3.4. Wind speed prediction results

Figure 8 shows the comparison between the predicted wind speed and the actual value in the next six hours in Weiyuan, China. The predicted wind speed is consistent with the actual wind speed. When the wind speed changes suddenly, the error between the predicted and real values is significant, and a lag effect between the predicted and real values is observed. Once the wind speed changes, the residual value at the current time suddenly increases, thus the predicted value at the next time changes accordingly due to the inherent characteristics of the time series model.

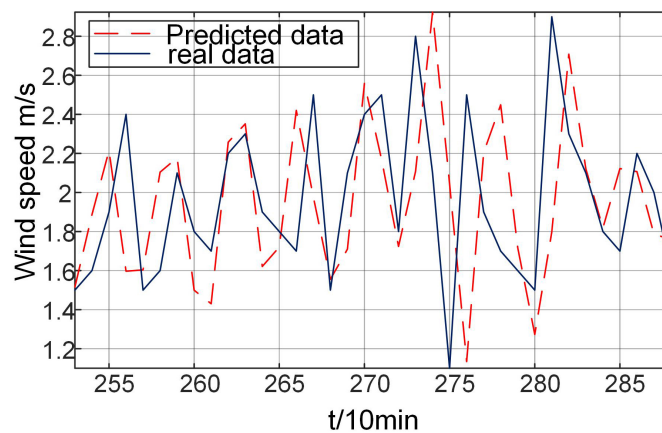


Fig. 8. Comparison of 6-hour wind speed prediction results and real values in Weiyuan area

6.4. Short term (emergency) dynamic capacity increase of traction network

Before the 253rd wind speed acquisition time, the traction network is assumed to pass through an 1158 A current (i.e., comprehensive current-carrying capacity of the traction network limited by the current technical regulations in Table 2), and the locomotive maintains steady-state operation under actual meteorological conditions. Under this condition, the operating temperatures of the messenger line, contact line, and reinforcement line are 40°, 28°, and 24°, respectively, so when the wind speed in the next six hours is the predicted value, the minimum meteorological value of the current month in Weiyuan, China, is taken for other geographical and climatic conditions (a wind direction coefficient of 0.8549 ambient temperature at -10.3°C and a unit radiation heat absorption power of 18.05 W/m). The relationship between the peak temperature and current of each transmission line at an altitude of 2174 m is shown in Fig. 9.

Figure 9 illustrates that the peak operating temperature of each transmission line increases with increased current. When the messenger line reaches its maximum allowable temperature of 95°C, the other transmission lines are far lower than their heat capacity limit. Figure 9 also shows that the maximum allowable operating current-carrying capacity of the messenger line in the next 6 hours is 532.4 A at 95°C, and the comprehensive current-carrying capacity of the

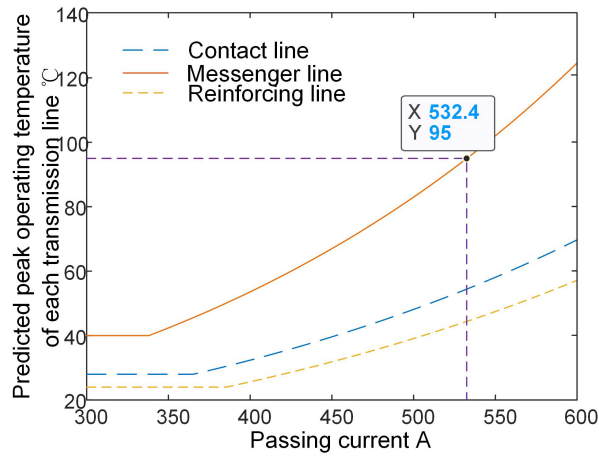


Fig. 9. Relationship between peak value of 6-hour temperature change curve and current of each transmission line under predicted wind speed

traction network is 1685 A. If the capacity of the traction network is increased according to the current-carrying capacity, the capacity is increased by about 45% compared with 1158 A and the effect is noticeable, as shown in Table 2.

To verify the reliability of the capacity increase limit of the traction network calculated by the calculation example, the predicted operation temperature change curve of each transmission line in the next six hours and the operation temperature change curve under the real wind speed in the next six hours are drawn through simulation when the messenger line passes through 532.4 A (with comprehensive current-carrying capacity of the traction network at 1685 A), as shown in Figs. 10(a) and 10(b).

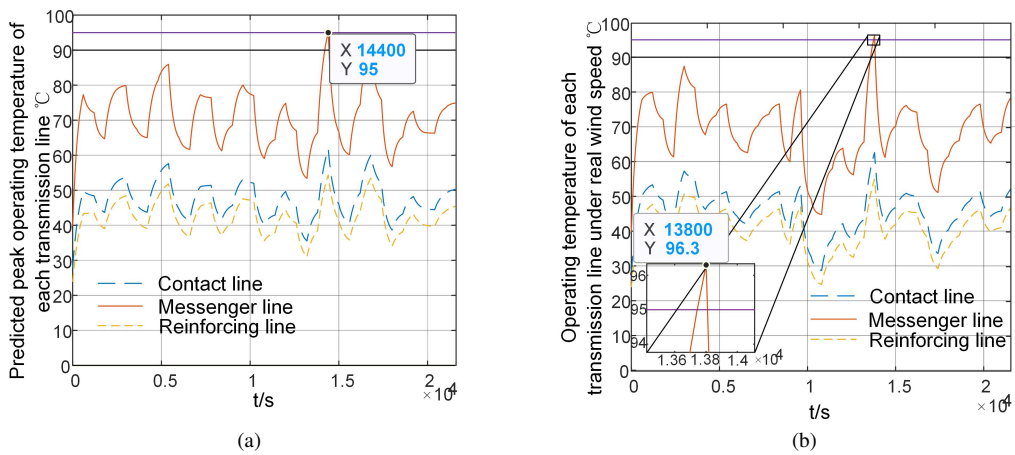


Fig. 10. Temperature change curve of each transmission line when the messenger line passes 532.4 A current in two condition: (a) at predicted wind speed; (b) at actual wind speed

Figure 10(a) shows that under the predicted wind speed when the messenger line passes through 532.4 A current (the comprehensive current-carrying capacity of the traction network at 1685 A), the operating temperature of each transmission line is lower than its temperature limit (95°C). However, as shown in Fig. 10(b), the operating temperature of each transmission line is also lower than the heat capacity limit (95°C) in actual wind speed. Therefore, the maximum operating temperature of the messenger line under the actual wind speed (96.3°C) is slightly higher than the maximum allowable operating temperature (95°C) in a short time due to the wind speed prediction error. In this case, it can be avoided by appropriately reducing the capacity expansion capacity of the traction network.

Because the traction network has a long-distance and span power supply, the change in wind speed is different across regions. Given this feature, dividing the capacity increase section into multiple grid points on average is only necessary. The meteorological monitoring device near the grid points can be used to measure wind speed. No meteorological monitoring device near some grid points may be noticed. The wind speed measurement sensor can be placed on these grid points to measure the wind speed. When evaluating the traction network's capacity increase limit, the traction network's comprehensive current-carrying capacity for each grid point is calculated. The minimum value is taken as the capacity increase limit in the traction network increase capacity section.

7. Conclusions

In this study, a dynamic capacity increase method of the traction network was proposed to improve the comprehensive current-carrying capacity of the traction network. The specific conclusions are as follows:

1. The operating temperature of the transmission line in the traction network is affected by geographical and climatic factors. Thus, can be used to dynamically increase the capacity of the traction network and tap the transmission potential. However, because the capacity-increasing process of the traction network is affected by the time-varying characteristics of model parameters, especially the wind speed, the impact on the comprehensive current-carrying capacity of the traction network is undeniable. Therefore, the effect of the time-varying characteristics of wind speed on the capacity growing traction process network must be considered during the process of dynamic capacity increasing.
2. The time series model has the advantage of not considering background information, simple modelling and less calculation. Although delayed, the requirements of practical evaluation of short-term capacity increase the limit of the traction network. Thus, more suitable for a traction power supply section with slow wind speed change. The shorter the prediction time, the higher the prediction accuracy.
3. The dynamic capacity increase method of the traction network based on wind speed prediction can effectively estimate the capacity increase limit of the traction network in a short term, avoid the impact of wind speed change on the capacity increase reliability of the traction network and ensure safety while significantly improving the transmission capacity of the traction network.

4. The rational use of dynamic capacity increase technology is helpful in improving the utilisation rate of the transmission line capacity of the traction network and improve railway operation efficiency, especially for short-term emergency dispatching.

Appendix A

Table A.1. Models and parameters of transmission lines

Transmission line name	Model	Equivalent radius (mm)	Unit mass (kg/km)	Specific heat capacity (J/kg/°C)	Resistance temperature coefficient (°C ⁻¹)	DC resistance at reference temperature 20°C (Ω/km)	Maximum allowable temperature (°C)	Limit temperature (°C)
Contact line j	CTAH120	6.18	1082	367	0.0038	0.147	95	200
Messenger line c	JTMH95	5.50	849	328	0.0027	0.231	95	200
Reinforcing line r	LGJ 185/30	9.03	774	732	0.0036	0.163	90	150

Table A.2. Meteorological parameters of Weiyuan in China

Parameter name	Symbol	Value	Unit
Wind speed	V_w	1.5	m/s
Wind direction angle	F_y	45	deg
Ambient temperature	T_a	-10.3	°C
Reference temperature	T_d	20	°C
Emissivity	ε	0.5	–
Radiant heat absorption power	P_s	18.05	W/m
Altitude	H_e	2174	m

Table A.3. Model parameters of time series model

Parameter	φ_1	φ_2	φ_3	φ_4	θ_1	θ_2	θ_3	θ_4
Value	-1.6156	1.4409	-1.5861	0.7609	-1.1400	1.1489	-1.2143	0.2789

Acknowledgements

This work was supported in part by the National Natural Science Foundation of China (Grant No. 52167013), in part by the Science and Technology Program of Gansu Province, China (Grant No. 17JR5RA083), and by the Program for Excellent Team of Scientific Research in Lanzhou Jiaotong University, China (Grant No. 201701).

References

- [1] Arroyo A., Castro P., Manana M., Domingo R., Laso A., *CO₂ footprint reduction and efficiency increase using the dynamic rate in overhead powerlines connected to wind farms*, Applied Thermal Engineering, vol. 130, pp. 1156–1162 (2018), DOI: [10.1016/j.applthermaleng.2017.11.095](https://doi.org/10.1016/j.applthermaleng.2017.11.095).
- [2] Sheng G., Qian Y., Luo L., Liu Y., Jiang X., *Key Technologies and Application Prospects for Operation and Maintenance of Power Equipment in New Type Power System*, High Voltage Engineering, vol. 47, no. 9, pp. 3072–3084 (2021), DOI: [10.13336/j.1003-6520.hve.20211258](https://doi.org/10.13336/j.1003-6520.hve.20211258).
- [3] Zhang Q., Qian Z., *Study on Real-Time Dynamic Capacity-Increase of Transmission Line*, Power System Technology, vol. 19, pp. 48–51 (2005), DOI: [10.3969/j.issn.1001-9529.2005.07.001](https://doi.org/10.3969/j.issn.1001-9529.2005.07.001).
- [4] Sun L., Zhang R., Tian M., Zhang H., Wang L., *Calculation Method of Permissible Carrying Capacity of OCS Considering the Influence of Geographical and Climatic Factors and its Application*, Power System Technology, vol. 45, no. 5, pp. 1958–1966 (2021), DOI: [10.13335/j.1000-3673.pst.2020.0740](https://doi.org/10.13335/j.1000-3673.pst.2020.0740).
- [5] Yan H., Wang Y., Zhou X., Liang L., Yin Z., Wang W., *Dynamic thermal rating of overhead transmission lines based on GRAPES numerical weather forecast*, Journal of Information Processing Systems, vol. 15, no. 4, pp. 724–736 (2019), DOI: [10.3745/JIPS.04.0122](https://doi.org/10.3745/JIPS.04.0122).
- [6] Fu S., Cai F., Wang M., Jin X., Zhang Q., Han X., *Dynamic capacity increase method of overhead line using practical regional weather data*, Electric Power Automation Equipment, vol. 41, no. 2, pp. 207–212 (2021), DOI: [10.16081/j.epae.202012020](https://doi.org/10.16081/j.epae.202012020).
- [7] Ma L., *Development of Artificial Intelligence Technology in Weather Forecast*, Advances in Earth Science, vol. 35, no. 6, pp. 551–560 (2020), DOI: [10.11867/j.issn.1001-8166.2020.053](https://doi.org/10.11867/j.issn.1001-8166.2020.053).
- [8] Yu M., Zhu J., Yang L., *Short-term load prediction model combining FEW and IHS algorithm*, Archives of Electrical Engineering, vol. 68, no. 4, pp. 907–923 (2019), DOI: [10.24425/ae.2019.130691](https://doi.org/10.24425/ae.2019.130691).
- [9] Zhang J., Wu M., *Calculation method of OCS ampacity for electric railway*, Journal of China Railway Society, vol. 37, no. 12, pp. 40–45 (2015), DOI: [10.3969/j.issn.10018360.2015.12.007](https://doi.org/10.3969/j.issn.10018360.2015.12.007).
- [10] Li Q., He J., *Analysis of traction power supply system*, Chengdu: Southwest Jiaotong University Press (2007).
- [11] *IEEE Standard for Calculating the Current-Temperature Relationship of Bare Overhead Conductors*, IEEE Std 738–2012 (Revision of IEEE Std 738-2006 – Incorporates IEEE Std 738-2012 Cor 1-2013) (2013).
- [12] Zhan J., Chung C.Y., Demeter E., *Time Series Modeling for Dynamic Thermal Rating of Overhead Lines*, IEEE Transactions on Power Systems, vol. 32, no. 3, pp. 2172–2182 (2017), DOI: [10.1109/TPWRS.2016.2596285](https://doi.org/10.1109/TPWRS.2016.2596285).
- [13] Liu Z., Deng H., Peng R., Peng X., Wang R., Zheng W., Wang P., Guo D., Liu G., *An Equivalent Heat Transfer Model Instead of Wind Speed Measuring for Dynamic Thermal Rating of Transmission Lines*, Energies, vol. 13, no. 18, 4679 (2020), DOI: [10.3390/en13184679](https://doi.org/10.3390/en13184679).
- [14] Meng T., Zhang H., *Wind speed short-term forecast for wind farms based on ARIMA model*, Science Technology and Engineering, vol. 13, no. 33, pp. 9813–9818 (2013).
- [15] Zhang S., Zeng J., Zhang H., Wang J., *Application of time series model to prediction of wind speed in wind field*, Water Resources and Hydropower Engineering, vol. 47, no. 12, pp. 132–135 (2016).

- [16] Ding T., Feng D., Lin X., Chen J., Chen L., *Ultra-short-term wind speed forecasting based on improved ARIMA-GARCH model*, Power System Technology, vol. 41, no. 6, pp. 1808–1814 (2017), DOI: [10.13335/j.1000-3673.pst.2016.2357](https://doi.org/10.13335/j.1000-3673.pst.2016.2357).
- [17] Bumham K.P., Anderson D.R., *Multimodel inference understanding AIC and BIC in model selection*, Sociological Methods and Research (2004).
- [18] Tangirala A.K., *Principles of System Identification: Theory and Practice*, Boca Raton, FL, USA: CRC Press (2015).